SEASONAL VARIATIONS of THE MLT TIDES IN 120°E MERIDIAN

Zeyu Chen and Daren Lu
Institute of Atmospheric Physics / Chinese Academy of Sciences

The SABER/TIMED temperature measurements covering November 2004 to January 2006 were used.

Application of Fourier-least-squares fit and FFT analysis with the data delineated the tidal harmonics. Tidal harmonics were composited to derive the tidal variations at the meridian at 120°E.

The seasonal variations of the major atmospheric tides in the mesosphere and lower thermosphere (MLT) region in the meridian were examined.

Motivations

Atmospheric thermal tides are global scale waves with periods as the sub-harmonics of a solar day (24 hrs). They are the global responses of the atmosphere to the diurnal heating from the heating agents that absorb solar irradiance, e.g., the tropospheric water vapor and the stratospheric ozone (Lindzen, 1967). For zonal homogeneous heating agents, the apparent westward motion of the Sun‘s illumination produces tides traveling at the same speed of the Sun, thus are nominated migrating tides. Chapman and Lindzen (1970) suggests the presence of nonmigrating tides due to longitudinally varying heating agents. After generated at lower altitude, atmospheric tides propagate upward with their amplitude increasing with altitude, then contribute substantially to the perturbations in the thermal and dynamical state in mesosphere and lower thermosphere region (MLT). While migrating tides are predominant in the MLT region, nonmigrating tides are important as they are considered to be responsible for the substantial longitudinal variations in the tides of prevailant frequencies, e.g., diurnal and semidiurnal tides (Khattatov et al, 1996; Hagan et al., 1997).

Satellite based monitoring of the atmosphere can provide measurements with global coverage. These enable tides retrieval with unambiguously delineating tidal harmonics both in temporal and spatial aspects (Hitchman and

Leovy, 1985; Brownscombe et al., 1985). Using the temperature measurements taken by the ISAMS/UARS (Improved Stratospheric and Mesospheric Sounder on board the UARS satellite, Dudhia et al., 1993), a maximum diurnal amplitude of 5K at equator is seen in the stratosphere and mesosphere. Using wind measurements from two instruments on board the UARS, i.e., the HRDI and WINDII, global tidal signals in MLT winds have been acquired extensive investigation (Hays et al, 1994; McLandress et al., 1996; Talaat and Lieberman, 1999).

In a small body of MLT tides research in China decades ago, Chen (1979a) conducts an in-depth investigation on the property of the differential operator of thermospheric tides, where the effect of mean wind and wind shear are all taken into account in deriving the operator. Using Miller's method (parabolic iteration), Chen (1979b) develops an numerical approach to solve the eignvalue-eignfunction problem, obtains the eignvalues and the coefficients for building the Hough functions for (1, 1) tidal mode.

In the past decade, substantial improvements in deploying ground-based wind profiler for monitoring MLT winds has been made (Chen et al., 2006), which leads to the presence of a number of estimations of MLT tides at Wuhan (30°N, 114°E). For example, the estimates of MLT wind tides by using meteor radar data are reported in Xiong et al. (2003) and in Zhao et al. (2005), and that using medium-frequency radar data are reported in Zhang et al. (2003) and Liu et al. (2006).

Currently, to improve the capability of monitoring aeronomy and space environment over China sector, a China national project, the Meridian project, has been being launched for establishing a ground-based observation station chain along the meridian at 120°E. The chain will substantially improve the situation of global monitoring of the state of the middle and upper atmosphere.

Nevertheless, the current knowledge of the general features of MLT tides over China sector is sparse, which led the current authors to conduct a comprehensive investigation revealing the features. Placing focus on the behavior of MLT tides in the meridian at 120°E, the authors reconstructed the MLT temperature tides of three leading frequencies, i.e., diurnal, semidiurnal and terdiurnal, in the meridian. In the research, global MLT temperature tidal harmonics were extracted from the temperature measurements over one year period taken by the SABER instrument on board the TIMED satellite.

DATA AND METHOD

- The TIMED satellite was launched on December 7, 2001. It flies in a nearly circular 625-km altitude orbit with an inclination of 74°, completes 15 orbits per day. The SABER/TIMED scans the limb emission of the atmosphere in 10 broadband spectral channels ranging 1.27-17 micrometer.
- It provides kinetic temperatures (Tk) that are retrieved from limb emissions at 15-micrometer CO2 band for daytime and combining the limb emissions at 4.3-micrometer CO2 band for nighttime.
- The L2A data-set of version 1.06 is used in the current research, and is publicly accessible from internet at http://saber.larc.nasa.gov.

- Using these harmonics, the tides in the 120°E Meridian were reconstructed. And the seasonal variations in the amplitudes of each kind of tides were observed. Particularly, the contribution of migrating and nonmigrating tides were payed substantial considerations. Through comparing with the wind tide estimates previously obtained by using the ground-based measurements at Wuhan locating at just near the meridian, general consistency was seen in the style of seasonal activity implied by the amplitudes.

DATA AND METHOD

- The current procedures of extracting tidal harmonics are the same as that used in the previous investigations (e.g., in McLandress et al., 1996, Forbes and Wu, 2003).
  - Fourier-leastsquares fit and the FFT analysis to delineate frequency and zonal wavenumber harmonics
- Binning scheme to build a composite data-set that provides not only global coverage but also the coverage of a full cycle of solar day in term of the LST at a geo-locations, which is available for the satellite that operates in longitudinally precessing mode, such as the TIMED.
  - The SABER/TIMED measurements precess in LST about 12-min every day. Thus, measurements in all the ascending tracks in 60 continuous calendar days can provide the data-set (hereafter referred to as 60-day data-set) covering a half solar day (12 hrs in LST), as is the case for the measurements in descending tracks. The measurements taken both in ascending and descending tracks in the 60-days cover a full solar day (24 hrs in LST).
  - All the 60-day data-sets in 2005 were selected from the SABER temperature measurements obtained during Dec. 2 in 2004 to Jan. 29 in 2006. Each 60-day data-set was denoted by the date of the 31st day in the data-set in term of the day of year (DOY). For example, the first 60-day data-set denoted by DOY1 consists the calendar days from Dec. 2 in 2004 to Jan. 31 in 2005.
  - Figure 1 shows for 2005 the LST coverage (hr) of each 60-day data-set with respect to latitude. Except for the situation at higher latitude where LST coverage is insufficient for extracting diurnal variations, LST coverage are longer than 20 hrs in the latitude range from 40°S to 40°N, which provide the possibility of delineating all the diurnal sub-harmonics. Thus, all the investigation in the current research were carried out in the latitude range.

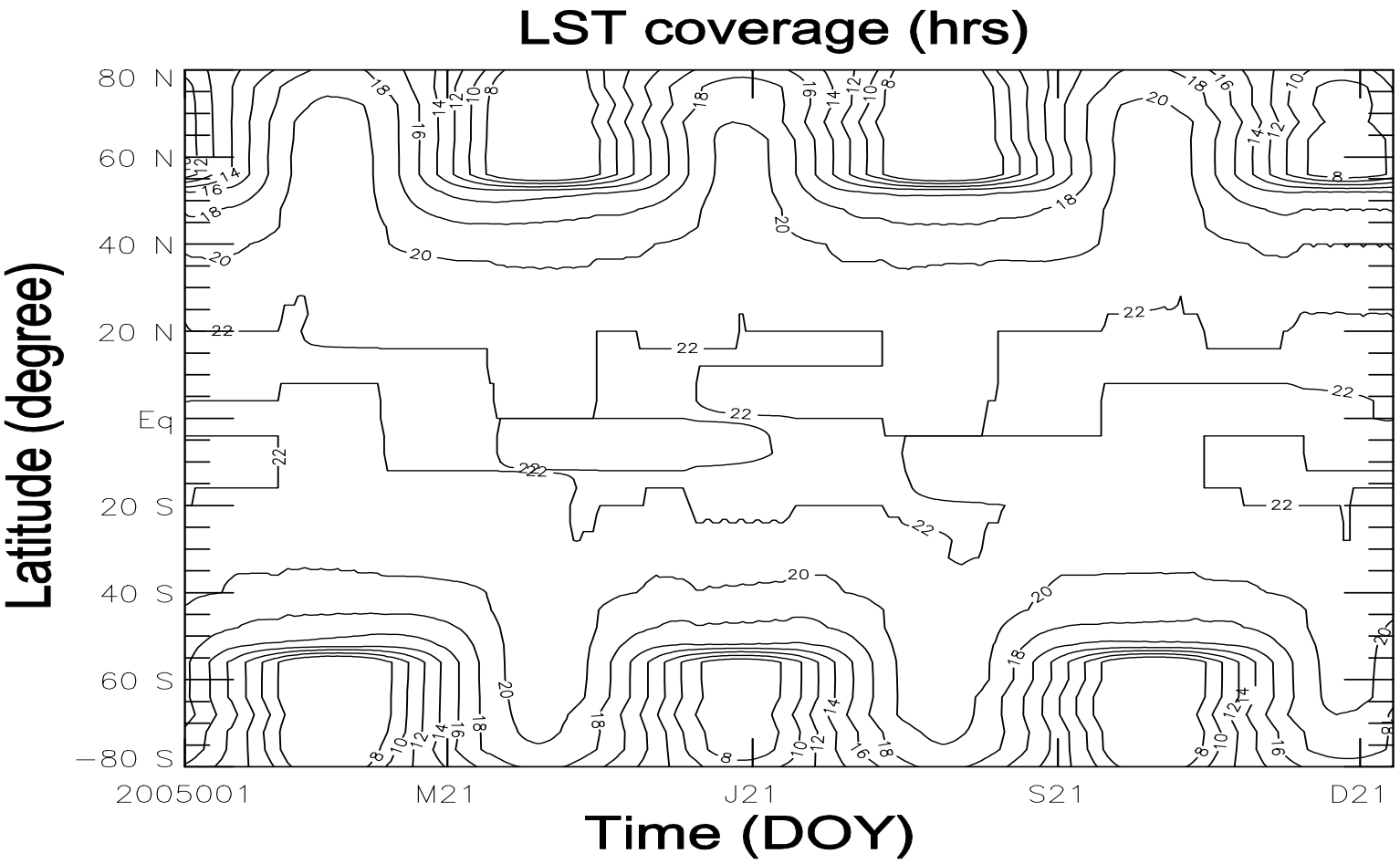

Fig. 1 Variation of LST (Local Solar Time) coverage (hr) with respect to latitude (negative for southern hemisphere) and date (Day Of Year, DOY) for all the 60-day bins obtained in 2005. Horizontal and vertical coordinate are for date and latitude, respectively, and 2005001 is for DOY = 0 in year 2005; Contour interval is 2 hr.

Main results

- Confined within latitude range from 40°S to 40°N, the migrating diurnal tide was the most predominant one in the whole MLT region at the meridian.
- Although with relatively weaker amplitude, all other tidal components exhibit significant amplitude at 97-km height. The primary features of the tidal variations were reflected by their respective tides at a reference height level at 97-km.
- Figure 2a shows the amplitude with respect to latitude and height of (1, 1) tide over March Equinox. Figure 2b and c are the amplitude of the tide over June and Winter Solstice, respectively. The migrating diurnal tides exhibit significant amplitude from 60 km altitude and reach maximum at 97 km, then the amplitudes decrease with altitude rapidly in the vertical. Moreover, Figure 2 shows that (1, 1) tide is most prominent in Equatorial area, and the latitude-height distribution of the amplitude is correlated with the position of the Sun. In March equinox (Figure 2a), the amplitudes are symmetric to the Equator. In the other two solstitial time, the amplitudes exhibit asymmetric distribution with respect to the Equator, the amplitude maxima tilts poleward with increasing altitude, towards the North Pole in summer and the South Pole in winter. Clear difference in the amplitude maximum at 97 km between equinox and solstice is seen in Figure 2.

- Using UARS wind measurements, the phenomenon has already been reported in the previous global tides analysis including numerical simulation study with the GSWM model, which leads Yudin et al. (1997) to conduct numerical sensitivity test, they suggests that the seasonally varying dissipation in mesopause region can account for the difference of (1, 1) mode amplitude.

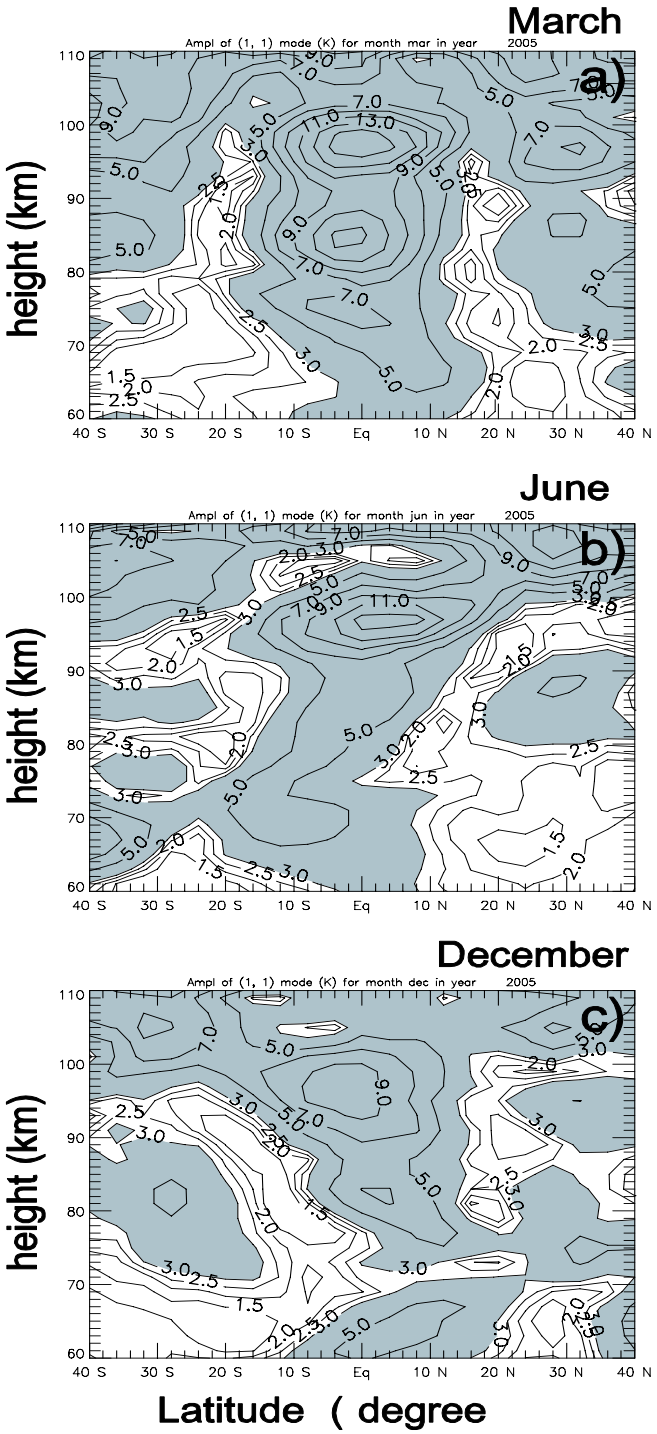

Fig. 2 Latitude-Height variation of the amplitudes (K) of migrating diurnal component, (1, 1) mode, during Spring equinox (a), summer solstice (b) and Winter solstice. Horizontal and vertical coordinates are latitude (degree, negative for southern hemisphere)
and height (km), respectively. All the Panels use the same contours with minimum of 2K.

Expression of tidal variations

$$\sum_{\substack{n=1,2,3 \\ m=-6,\ldots,+6}} A\cos\left(n\omega t + m\lambda - \phi\right)$$

n: frequency,

omega, angular speed of the rotation of the earth

m: zonal wavenumber

ϕ : initial phase, can be converted to the LST (hr)

- n = 1 diurnal
- n = 2 semi-diurnal
- n = 3 ter-diurnal

m = -6 …… +6，

m > 0 propagating westward

m < 0 propagating eastward

Migrating component: n = m

Non-migrating component: n ≠ m

Seasonal variations of the MLT tides at the Meridian

Focusing on a specific meridian, diurnal tides can be evaluated by setting n=1 and the longitude value 120E where the meridian locates, as shown in the following:

$$T_{diurn} = \sum_{\substack{n=1 \\ m=-6,\ldots,+6}} A\cos\left(\omega t + m\lambda - \phi\right)$$

$$n = 1, \lambda = 120\,^{\circ}E$$

The procedure will generate a sinusoidal time series (T_{diurn}) with period of one solar day. The maximum in the series is chosen as the amplitude of the diurnal tides, and the corresponding time the phase.

Main results– Diurnal tidal variations at 97-km, the reference height

Figure 3a shows the seasonal variations in the amplitudes of the diurnal temperature tides (T_{diur}) at 97 km over 40S to 40N.

- The migrating component plays dominant role in characterizing the general features of both of the diurnal and the semidiurnal tides.
- The migrating diurnal tide is the most predominant tidal perturbations. It is most active during March equinox, which is characterized by the amplitude maxima at the equator and that at the tropics for both hemispheres.
- The predominance of the migrating semidiurnal tide occurs at tropical latitudes for both hemispheres. In the northern hemisphere, the tide exhibits intense amplitudes during September equinox with a maximum of 13K. In the southern hemisphere, it is intense in between March equinox and June solstice.

Fig. 3 Seasonal and latitudinal distribution of the amplitude of diurnal tides (a), migrating diurnal tides (b) and non-migrating diurnal tides (c) at the 97-km altitude in the meridian at 120°E from 40°S to 40°N in 2005. Horizontal and vertical coordinate are date (DOY) and latitude, respectively; M21, J21, S21 and D21 are the same as that in Fig. 1. All Panels use same contours with a minimum of 2 K， and where the amplitudes greater than or equal to 5 K are shaded.

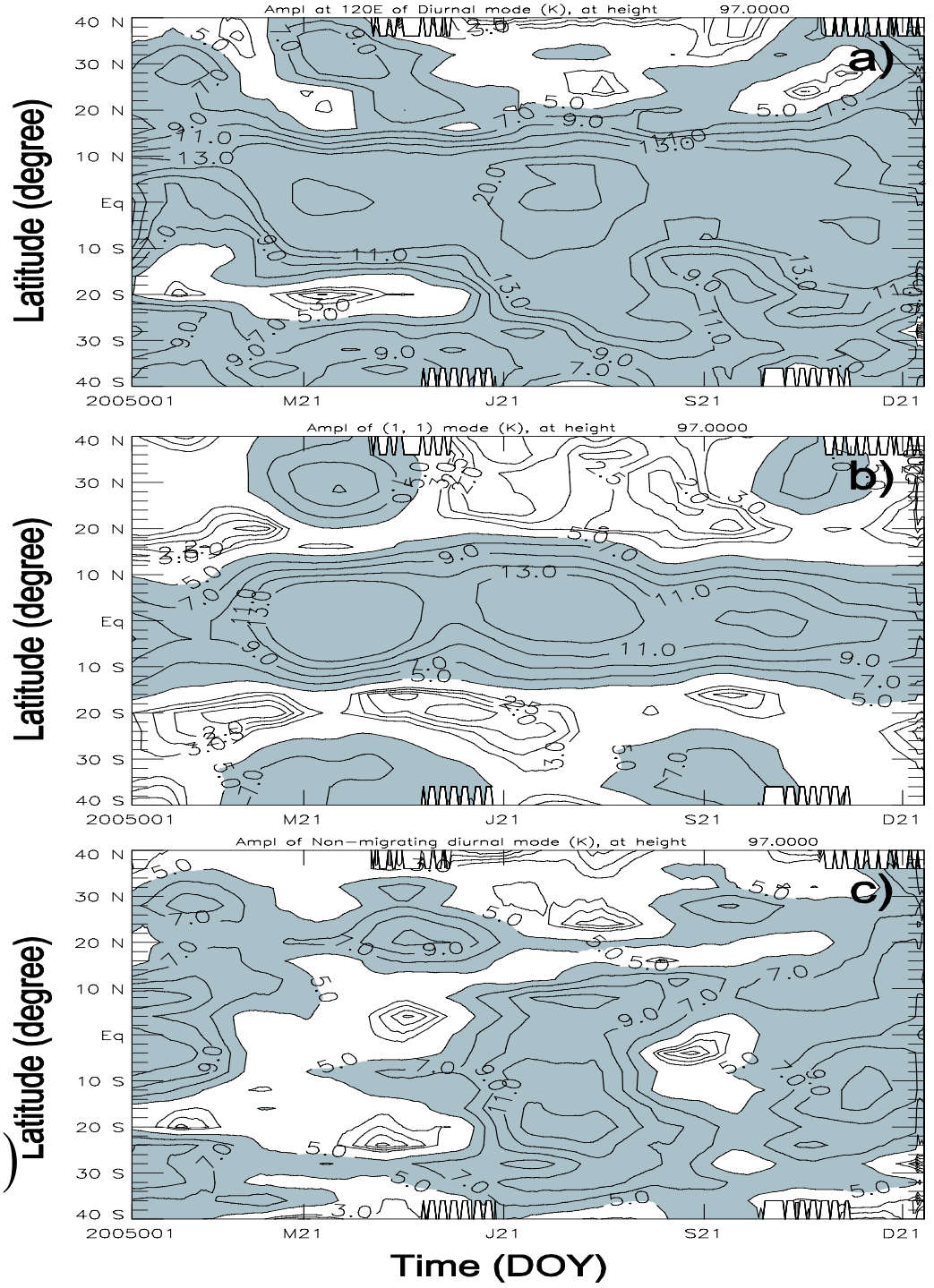

The non-migrating tides contain the contribution from all the tidal components except the migrating component.

$$T_{non-migra} = \sum_{\substack{n=1 \\ m=-6,..,0,2,.,+6}} A\cos\left(n\omega t + m\lambda - \phi\right)$$

Contribution from the non-migrating components

Figure 3c indicates that the nonmigrating component also contribute substantially to the full diurnal tides. In Figure 3c, the area with amplitude greater than or equal to 5K that exceeds the measurement accuracy (2K at the altitude) are shaded. It is seen in Figure 3c that during most time in the year, nonmigrating tides exhibit prominent amplitude at the tropical area. During summer solstial time, nonmigrating tides are intense in the latitude cycles from 10°N to 30°S. Particularly, at 20°S, extreme amplitude exceeding 13 K is seen. The influence of nonmigrating tides during the period results in the maximum amplitude of 20 K that appears at the Equator (Figure 3a). Meanwhile, the the extreme large amplitudes at 20°S results in the Equatorial maximal amplitude extending southward, see the area covered by the 13-K contour in Figure 3a.

Moreover, each diurnal harmonics contributing to the final apparent nonmigrating tides were examined, and the results indicated that (1, 0), (1, 2) and (1, -3) are the important modes due to their significant amplitude. While this has already been reported in the past researches, the current investigation revealed an additional prominent diurnal harmonic, (1, -2) mode, which mode show amplitude comparable to that of (1, 0) mode. The amplitude at 97-km height for all these four diurnal harmonics are presented in Figure 4.

Examining with detail the Panel in Figure 4, it is found that (1, 2) mode and (1, -3) mode are of most important by their amplitudes, and that (1, 0) and (1, -2) mode are weaker. Figure 4b and c show that the maximum amplitude of (1, 2) and (1, -3) modes are greater than 7 K. Figure 4c further indicates that during summer solstice, the amplitude of (1, -3) mode reaches a maximum greater than 9 K. Recalling that the nonmigrating tides shown in Figure 3c reflect the superposition of these harmonics, the amplitude maxima in (1, 2) mode (Figure 4b) and (1, 3) mode (Figure 4c), both occurring near concurrently at the tropics in Southern hemisphere, can accounts for the occurrence of the intense nonmigrating tides appearing in the same period in the Southern tropical area at 20°S (Figure 3c).

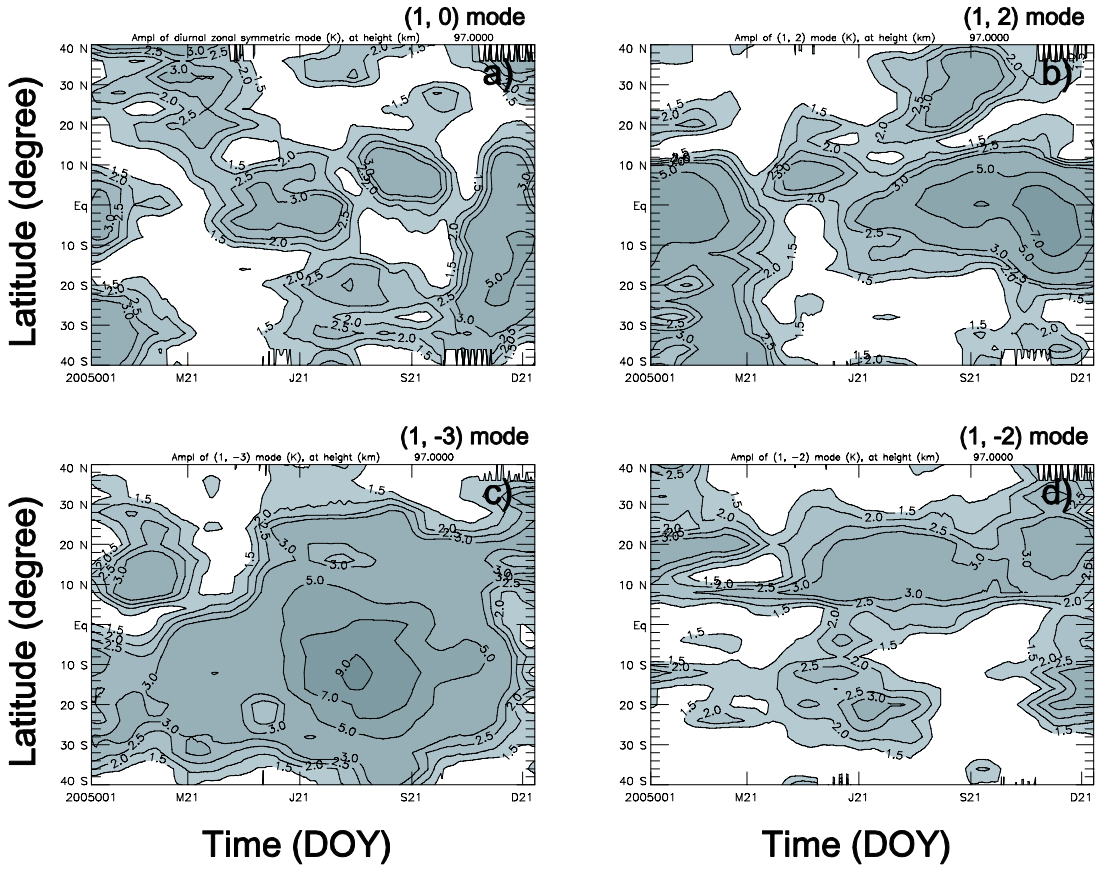

Fig. 4 Seasonal and latitudinal distribution of the amplitude of the predominant nonmigrating diurnal modes at 97 km altitude in the meridian at 120 ° E in latitude range 40 ° S~40 ° N in 2005. The coordinates are the same as that in Fig. 3. All Panels use same contours with a minimum of 1.5 K and where the amplitudes grater than or equal to the minimum are shaded.

Meteor radar wind tides at Wuhan (31°N, 114°E)

Xiong et al., 2003

Diurnal amplitude
Left for U
Right for V

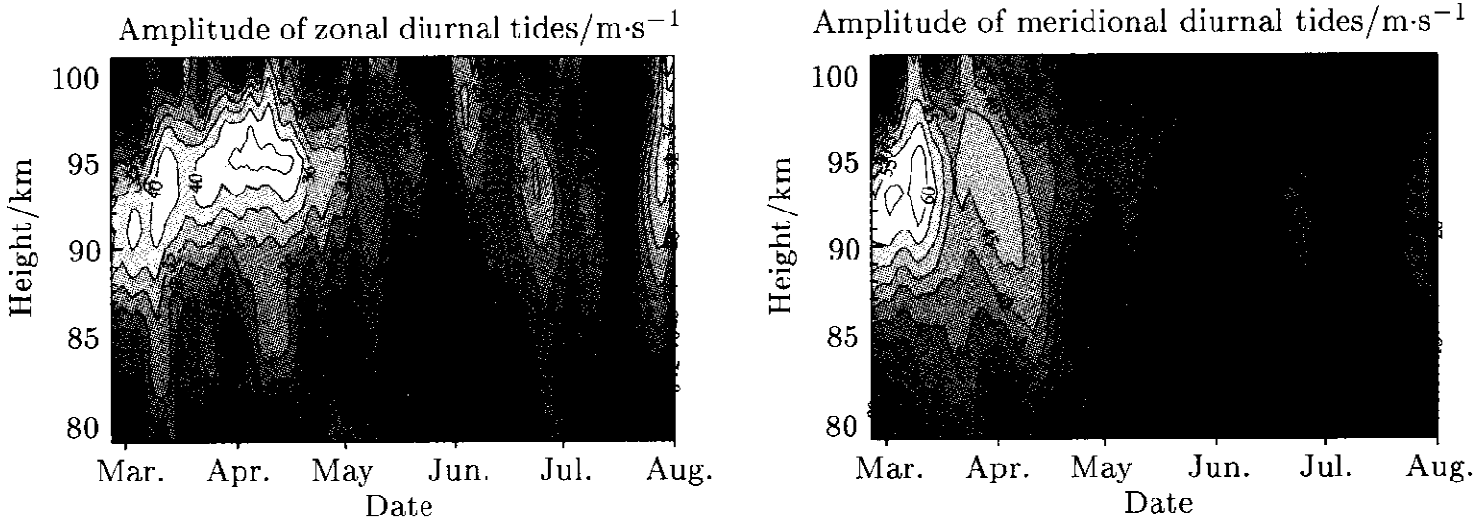

T_{diur} is in principle equivalent to those derived by using single site measurements, the amplitudes shown in Figure 3a were compared with the previous estimates of diurnal wind tides from the meteor radar winds at Wuhan.

Xiong et al.(2003) report that the diurnal wind tides at Wuhan during February to July in 2002 are significant over the altitude range 90-100 km, They exhibit intense amplitude only during spring time (March to April); in the meantime, diurnal meridional wind tides further exhibit sporadic large amplitudes during summer time. Although it is difficult to make point-point comparison between wind tides and temperature tides, the seasonal behavior of the diurnal tides at Wuhan-latitude among this shown in Figure 3a and that reported in Xiong et al.(2003)is consistent.

Semidiurnal variations during the year

The semi-diurnal tides is shown in Fig 5 (the right panels).Dominated by the migrating component, the semidiurnal tides exhibit maximal amplitudes in the tropics for both hemispheres, and are most prominent during that after March equinox, and that around September equinox. The tides in other seasons are influenced substantially by the non-migrating tides with weaker amplitudes.

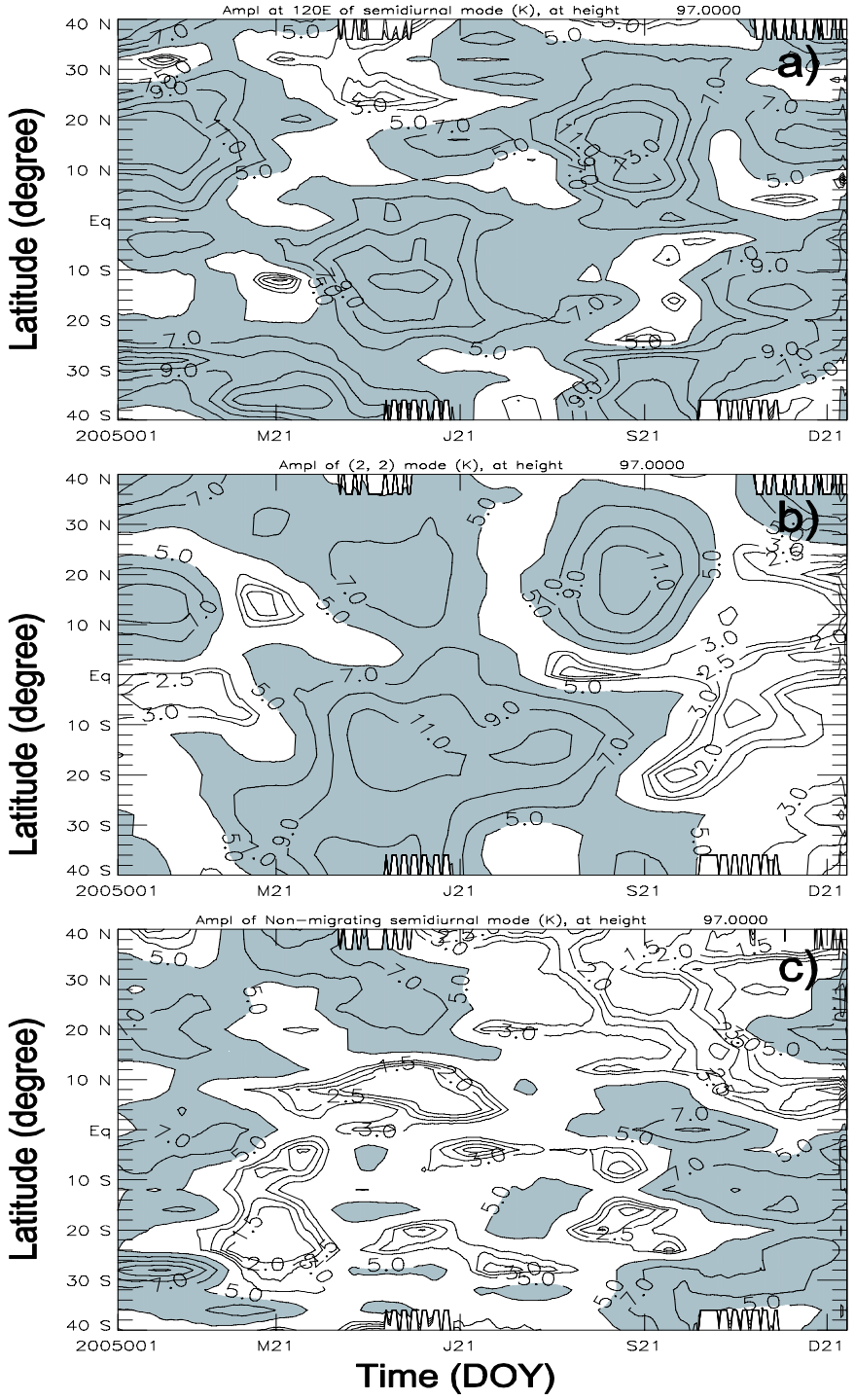

Fig. 5 Seasonal variations of the amplitude (K) of semidiurnal tides (a), migrating semidiurnal tides (b) and nonmigrating semidiurnal tides (c) at the 97-km altitude in the meridian at 120°E from 40°S to 40°N in 2005. The coordinates and the description of contours are the same as those in Fig. 3, respectively.

Ter-diurnal variations during the year

Confined in latitude range 40°S-40°N, all ter-diurnal tides exhibit much weak amplitudes. Moreover, the non-migrating tides are found to be with larger amplitude during many times than the migrating tide, although the later exhibit regular occurrence at the Equator.

Nevertheless, the current results suggested that the non-migrating tides are predominant during most times in 2005.

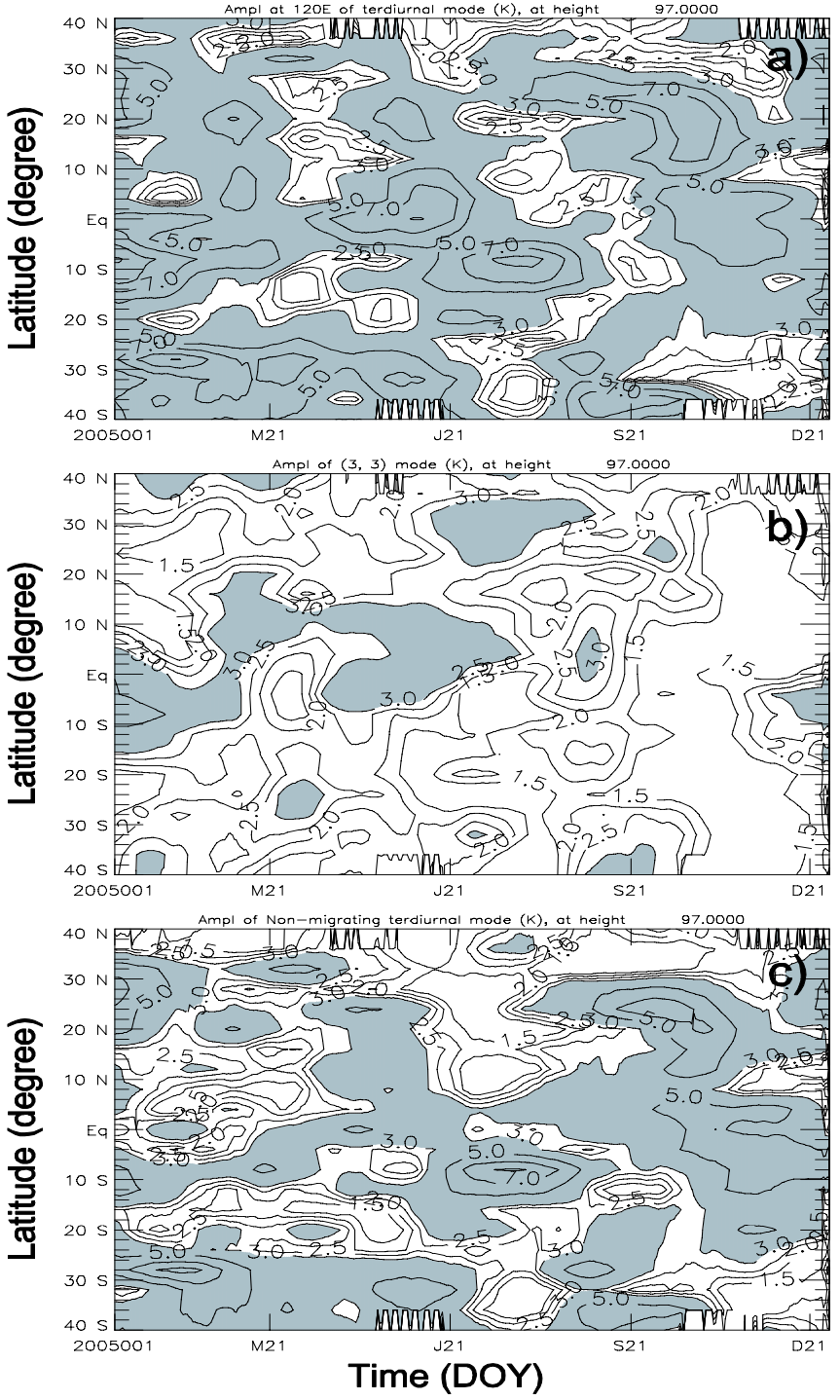

Fig. 6 Seasonal variations of the amplitude (K) of ter-diurnal tides (a), migrating ter-diurnal tide (b) and non-migrating ter-diurnal tides (c) at the 97-km altitude in the meridian at 120°E from 40°S to 40°N in 2005.

The coordinates and the description of contours are the same as those in Fig. 3, respectively; And the area with amplitudes greater than or equal to 3 K are shaded.

Summary

•The SABER/TIMED temperature measurements covering the year of 2005 were used to investigate the general features of the predominant MLT tides in the meridian at 120°E. Global tidal harmonics with respect to frequency n and zonal wavenumber s, (n, s) tide, were delineated by applying the Fourier-least-squares fit and the FFT analysis. Then, the harmonics were used to reconstruct the MLT tides at the meridian.

•The migrating tides predominate across the year both for diurnal and semidiurnal tides. The domination of (1, 1) tide is reflected by the amplitude maxima occurring at the Equator across the year, as well as the amplitude maxima in the subtropics for both hemispheres during Equinox.

•It was also found that (1, 0), (1, 2), (1, -3) and (1, -2) tidal modes are most prominent. Contributions from all these tidal modes result in intense non-migrating diurnal tides during summer solstitial time spanning over 20°N to 30°S. And the superposition of this maximum non-migrating tides and the migrating tides results in a maximum of 20-K amplitude in the whole diurnal tides seen at the Equator during summer solstitial time in the year, as is the extreme amplitude in the year.

•Dominated by the migrating component, the semidiurnal tides exhibit maximal amplitudes in the tropics for both hemispheres, and are most prominent during that after March equinox, and that around September equinox. The tides in other seasons are influenced substantially by the non-migrating tides with weaker amplitudes.
•Ter-diurnal harmonics were not as prominent as the diurnal and semi-diurnal tides in the latitude range 40°S to 40°N. Moreover, the results also indicated that the non-migrating tides predominate over the year, which shapes the primary spatial distribution of and temporal variations in the tides.

References

•Burrage et al., GRL, 1995, 22(19), 2641-2644.
•Chen et al., Chin. J. Space Sci., 2006, 26(Suppl), 61-70.
•Chen, Numerical calaulations of the eigenvalue-eigenfunction problem fror the diurnal mode of the atmospheric tide. ACTA Geophysica Sinica (in Chinese), 1979, 22(3), 237-242.
•Chen, The differential operator and integro-differential equation of the thermospheric tides. ACTA Geophysica Sinica (in Chinese), 1979, 22(4), 396-405.
•Dudhia et al., Geophys. Res. Lett., 1993, 20, 1251-1254.
•Hagan et al., Ann. Geophys., 1997, 15, 1176-1186.
•Hays et al., J. Atmos. Sci., 1994, 51, 3077-3093.
•Khattatov et al., JGR, 1996, 101, 10393-10404.
•Liu R et al., J. Atmos. Terr. Phys., 2006, 68, 1245-1259.
•McLandress et al., J. Geophys. Res., 1996, 101, 10, 441-10,453.
•Smith A K, Structure of the Terdiurnal Tide at 95 km, GRL, 27(2), 177-180, 2000.
•Talaat E R and Lieberman R S, J. Atmos. Sci., 1999, 56, 4073-4087.
•Xiong et al., Chin. J. Space Sci. (in Chinese), 2003, 23(5), 361-370.
•Yudin V A, Khattatov B V, Geller M A et al., Thermal tides and studies to tune the mechanistic tidal model using UARS observations. Ann. Geophys., 1997, 15, 1205-1220.
•Zhang et al., Chin. J. Space Sci. (in Chinese), 2003, 23(6)， 430-435.

Main results

- Particular focus was placed on investigating the contribution of non-migrating tides.
  - For diurnal variations, four non-migrating diurnal tidal components, i.e., (1, 0), (1, 2), (1, -3) and (1, -2), were found to contribute substantially to the diurnal tidal variations. These four tides contribute together during June solstice to form an area covering 10°N to 30°N with maximal amplitude 20K appearing at the Equator.
  - The influences of non-migrating semidiurnal tides appears clearly in other seasons, and a number of amplitude maxima are seen.
- Moreover, the reconstructed diurnal tidal variations were compared with the observational analysis using meteor radar wind measurements taken at Wuhan (30°N, 114°E), and significant consistency was seen in the comparison.